CHAPTER-2

A Novel P3HT/MoS_2 Nanocomposite-based Organic TFT for Ammonia Detection

2.1 Introduction 40
2.2 Chemical used and Material Synthesis 43
2.3 Device Fabrication Steps 43
2.4 Thin Film Characterization 45
2.5 Device Results and Sensing Mechanism 47
2.6 Electrical and Extracted Sensing Parameters 51
2.6.1. Evolution of Gas Response 51
2.6.2. Sensing Response and Selectivity 52
2.6.3. Detection Limit 52
2.6.4. Effect of Relative Humidity Variation 54
2.6.5. Qualitative Analysis 54
2.7 Sensing Mechanism 56
2.8 Conclusion 58

The part of the work is adopted from-

A. Verma, P. K. Sahu, V. Chaudhary, A. K. Singh, V. N. Mishra, and R. Prakash, "Fabrication and Characterization of P3HT/MoS_2 Thin-Film Based Ammonia Sensor Operated at Room Temperature," ***IEEE Sensors Journal***, vol. 22, no. 11, pp. 10361-10369, 1 June 1, 2022, ***doi: 10.1109/JSEN.2022.3170698***.

Abstract:

The composites of polymers and two-dimensional (2D) materials show promising applications in the area of gas sensing. In this work, we report an efficient ammonia gas (NH_3) sensor based on poly(3-hexylthiophene)/molybdenum disulfide (P3HT/MoS_2) nanocomposite. The sensing device has been fabricated in bottom-gate top contact organic thin film transistor (OTFT) assembly using P3HT/MoS_2 as active channel material. The changes in the electrical response of OTFT has been measured and analyzed for various ammonia gas concentration at room temperature. The sensing device in the form of an OTFT structure is preferred due to multi-parameter characteristics to explore gas sensing applications. The active sensing layer has been fabricated via a self-assembled, cost-effective floating film transfer (FTM) technique. An optimized uniform sensing film of thickness 25±3 nm is used to analyze the change in the electrical characteristic of the device in terms of I/O characteristics, mobility, threshold voltage, trapped charge density, etc., for various ammonia concentrations. The OTFT with nanofiber morphology of mobility 0.147 cm^2/V-s shows a threshold voltage of -3.78 V (in the air) and changes to -10.71 V after 100 ppm ammonia gas exposure. The device has shown a limit of detection (LOD) of 904 ppb and a sensing response of 63.45% at 100 ppm ammonia concentration. The extraction of multi-parameter sensing characteristics of the device has been conducted in a closed chamber with an ambient environment. The fabricated sensor is therefore having potential applications in high-performance ammonia sensing applications.

2.1 Introduction

Nowadays, NH_3 in the ambient has become a significant concern due to life-threatening

issues and indirect contribution to global warming [67][103]. Ammonia, a colorless toxic gas emitted from agricultural activity, livestock, diesel and petrol vehicles, etc., is very harmful to flora and fauna when it exceeds a specific limit [104]–[106]. The exposure of NH_3 over the defined limit (according to the Occupational Safety and Health Administration (OSHA), the maximum exposure time to 35 ppm for 15 min) may cause blindness, death, lung damage, coma, collapse, and seizures [105][107][108]. Therefore, the technological demand for efficient ammonia gas sensors is continuously increasing because of their potential application in humankind and environmental protection [17], [109], [110]. In the prevailing literature, ammonia sensing using various methods have been reported, such as metal oxide (MO) gas sensor, conducting polymer (CP) based gas sensor, tunable diode laser spectroscopy (TDLS), electrochemical gas sensor, surface acoustic wave (SAW) gas sensor, etc. The CP-based gas sensors have gained more attention due to their outstanding multi-parameter characteristics and versatile functionalities [17][111]. Recently, CP/(2D) materials have been a topic of interest in the field of gas sensing applications because of their versatile functionalities in terms of high sensitivity, high response, and room temperature (RT) operation [111]–[113]. Depending on the variety of applications, CPs can be used as an active layer for diodes or OTFTs fabrication [114]–[118]. The CP/2D nanocomposites envisage with high stability, sensitivity, low response/recovery time, low operating temperature (usually RT), etc., due to combining the advantage of both the CPs and 2D materials [112][119][120]. The CP or CP-based nanocomposites such as polyaniline (PANI), P3HT/polystyrene(PS), P3HT/MoS_2, Poly(3,3'"-didodecyl quarter thiophene)(PQT-12), pentacene, copper oxide (CuO)/ reduced graphene oxide (rGO), zinc oxide (ZnO)/polypyrrole (PPy), tungsten trioxide (WO_3), etc. [121]–[127] for ammonia sensing have been investigated in the literature. Furthermore, the

CPs viz. polythiophene (PTh), polypyrrole (PPy), PANI, PQT-12, and their derivatives as a sensing layer have gained more attention in the field of gas sensing due to their flexible nature, facile synthesis, low-cost, and eco-friendly advantages in fabrication process *[28]–[30].* Although CP-based sensors exhibit good sensitivity and room temperature operation, however, it suffers from a low response, poor stability, or less lifetime *[31].* Further, the sensing performance and stability of CP-based sensors can be enhanced by fabricating nano-composites with suitable filler materials and or by doping *[32][33].* The CP-based sensors are mostly chemiresistive types, requiring a transducer device to process electrical signals [74]. The PTh derivatives-based sensing layer, such as P3HT, PBTTT, and composites of PTh derivatives with 2D material, such as P3HT/MoS_2 materials, have outstanding properties to fabricate OTFT due to its enhanced current densities and better charge transport properties [17][134][135], fast processing, higher mobility, solution processible, and compatibility with various substrates (like polyethylene terephthalate (PET), glass, silicon, etc.) at reasonable cost [136]. Recently, P3HT/MoS_2 has been used in numerous applications because of its air-stable nature and higher mobility [137][138]. Previously, the polymer/2D composite material was utilized for NH_3 sensing by Tao Xie et al., where they utilized a spray coating technique to deposit a P3HT/MoS_2 active layer over SiO_2 substrate for OTFT fabrication [123].

Various methods have been reported for the deposition of CPs thin film, such as; dip casting, spin casting, vacuum deposition, Langmuir-Blodgett (LB) deposition, layer-by-layer self-assembly, and floating film transfer method (FTM), etc. [139]–[141] The FTM, a solu-tion processible method (shown in **Figure 1.5**), was demonstrated by Morita et al. for depo-sition of thin films for OTFTs, and later, this fabrication method was optimized for other thiophenes [142][143]. Here a thin floating polymer film is obtained over the liquid surface

to obtain a self-assembled monolayer (SAM) floating film due to the formation of polymer sol-gel and continually drawing viscous liquid force [144]. The sensing response for ammonia gas has been explored in this chapter utilizing P3HT/MoS_2 composite as a sensing layer deposited by the FTM technique.

2.2 Chemical used and Material Synthesis

The polymer P3HT (average molecular weight M_w; 54-75 kDa) and MoS_2 were bought from Sigma Aldrich, USA, and SPI supplies, USA, respectively. The chemical structure of poly(3-hexylthiophene) and molybdenum disulfide has been illustrated in **Figure 2.1(a)** and **Figure 2.1(b),** respectively. To obtain the desired P3HT/MoS_2 solution, 1 mg/ml of MoS_2 was dispersed in chloroform ($CHCl_3$) via sonification for 6 hr. at 30 kHz. Further, a 3 mg of P3HT was separately dispersed in 970 µl of chloroform at 50 °C for 1 hr., and then it was cooled to RT. After that, a 30 µl of MoS_2 dispersed solution was added to P3HT dispersed solution and again sonicated for 3 hr. to obtain a homogeneous dispersion of P3HT/MoS_2 with a concentration of 3 mg/ml. For depositing P3HT/MoS_2 active layer, a liquid substrate was prepared by mixing ethylene glycol ($C_2H_6O_2$) and glycerol ($C_3H_8O_3$) in a ratio of 3:1 and poured into a petri dish. Then around 15 µl of the composite solution was dropped at the center of the liquid surface to get FTM film. This film fabrication process is illustrated in **Figure 1.5**. During the growth of composite thin film, suitable precautions should be taken to avoid any anisotropy because the orientation and crystallinity of the floating film growth depend upon the deposition conditions in the FTM technique. The thickness of stumped P3HT/MoS_2 composite film was ~25 nm, measured by Reflectometer (F20-UV).

2.3 Device Fabrication Steps

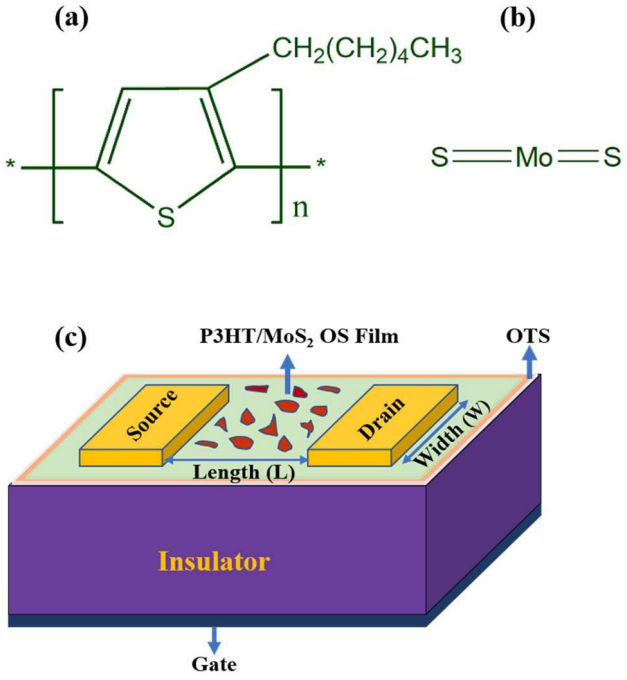

Figure 2.1 Chemical structure of (a) P3HT, (b) MoS_2, (c) Geometry of fabricated device.

The bottom gate top contact (BGTC) OTFT architecture, shown in **Figure 2.1(c)**, has been fabricated on a highly p-doped silicon wafer with a 300 nm SiO_2 layer. Before depositing P3HT/MoS_2 film, the substrate is treated with trichloro(octadecyl)silane (OTS) in toluene. The OTS-treated dielectric has shown oxide capacitance (C_{ox}) of 10 nF/cm^2. After that, the floating film of ~ 25 nm P3HT/MoS_2 nanocomposite film on the liquid substrate was carefully stumped on SiO_2/Si substrate for OTFT fabrication. Further, the obtained film was washed with methanol to remove the adhered hydrophilic property of the film and annealed at 60 °C to avoid any residuals (like $CHCl_3$ and methanol) on the prepared film. After that, the gold electrodes (drain and source) of thickness ~ 60 nm were deposited using a nickel shadow mask via thermal evaporation (HIND HIVAC) at a base pressure of ~10^{-6} Torr and deposition rate of ~1.5 Å/s. The width (W) and length (L) of the channel are 1 mm and 100 μm, respectively. The multi-parameter testing of the device is carried out by a semiconductor

device analyzer (Keysight B1500A).

2.4 Thin Film Characterization

The X-ray diffraction (XRD) of the synthesized film is carried out to examine interplanar spacing and the crystal orientation of the thin film. The Intensity vs. 2θ (degree) plot of pristine P3HT and P3HT/MoS_2 composite is shown in **Figure 2.2**. The pristine P3HT film exhibits a sharp (100) peak at 5.33° along with other minor peaks (200), (300) at 10.68 and 16.0, respectively [116]. On the other hand, P3HT/MoS_2 composite shows a sharp (100) peak corresponding to the lamellar structure of P3HT at 5.33° with other relatively sharp higher-order reflections (200) and (300) at 10.66° and 15.99°, respectively [117][118]. The appearance of sharp higher-order reflections corresponding to the lamellar structure of P3HT confirms the enhancement in the crystalline features of P3HT upon insertion of MoS_2.

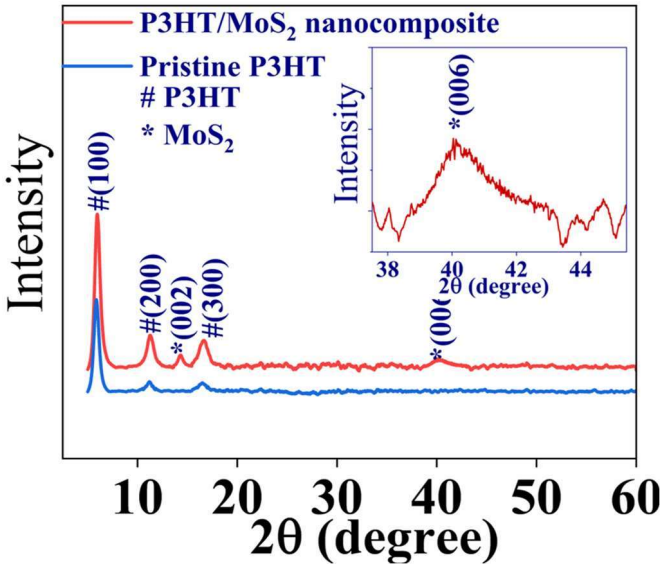

Figure 2.2 The XRD spectra of P3HT and P3HT/MoS_2 nanocomposite film.

Further, the diffraction peaks at 14.4º and 40.2° corresponding to the 2H phase of MoS_2 have also been observed in the composite sample [134][145]. It has been reported that mono/few-layer exfoliated MoS_2 nanosheets show (002), (006) diffraction planes at 14.4º and 40.2°

(shown in the inset of **Figure 2.2**), corresponding to the 2H phase of MoS_2 [145]. In general, in 2H-MoS_2 structure, the (002) and (006) planes demonstrate the interference of layered S–Mo–S and it's periodical progression along the c-axis in 2H symmetry. The (002), (006) peaks at 14.4° and 40.2° in P3HT/MoS_2 composite verify the presence of mono/few-layer MoS_2 in the composite film.

To observe the effect of MoS_2 on the ordering and interaction behavior of the polymer matrix chain, UV-Vis spectra has been recorded and is shown in **Figure 2.3(a)**. The pristine P3HT polymer film has shown one absorption peak at 450 nm. Moreover, the absorption spectra of the P3HT/MoS_2 nanocomposite have an absorption peak at 450 nm with two other prominent absorption peaks at 570 nm and 615 nm, attributed to A_{0-1} and A_{0-0} transitions, respectively (A represents the intensity of absorption). The appearance of two sharp peaks at 570 nm and 615 nm, indicates an enhancement in the P3HT crystallization and conjugation via MoS_2 material in P3HT/MoS_2 nanocomposites [134][146].

The atomic force microscopy (AFM) image of the synthesized film was carried out by AFM (NT-MDT, Russia, model PRO 47) under tapping mode. The AFM images of the P3HT/MoS_2 composite and pristine P3HT are shown in **Figure 2.3(b)**, and **Figure 2.3(c)**, respectively. The pristine P3HT has shown smoother morphology, as shown in **Figure 2.3(c)**, while P3HT/MoS_2 composite film has demonstrated the nanofiber morphology due to processing conditions and methodology adapted (**Figure 2.3(b)**). The domains in the pristine P3HT are uncoupled or separated, while P3HT/MoS_2 domains are coupled and form a nanofiber structure. The long-coupled nanofiber morphology in the polymer nanocomposite matrix creates an additional path for the charge transport facilities. Hence, the P3HT/MoS_2 composite film has superior morphology as compared to pristine P3HT film in terms of ammonia

gas sensing. The sensing of ammonia gas is carried out in the indigenously developed gas sensing chamber (volume of 10 L), as depicted in **Figure 2.3(d)**).

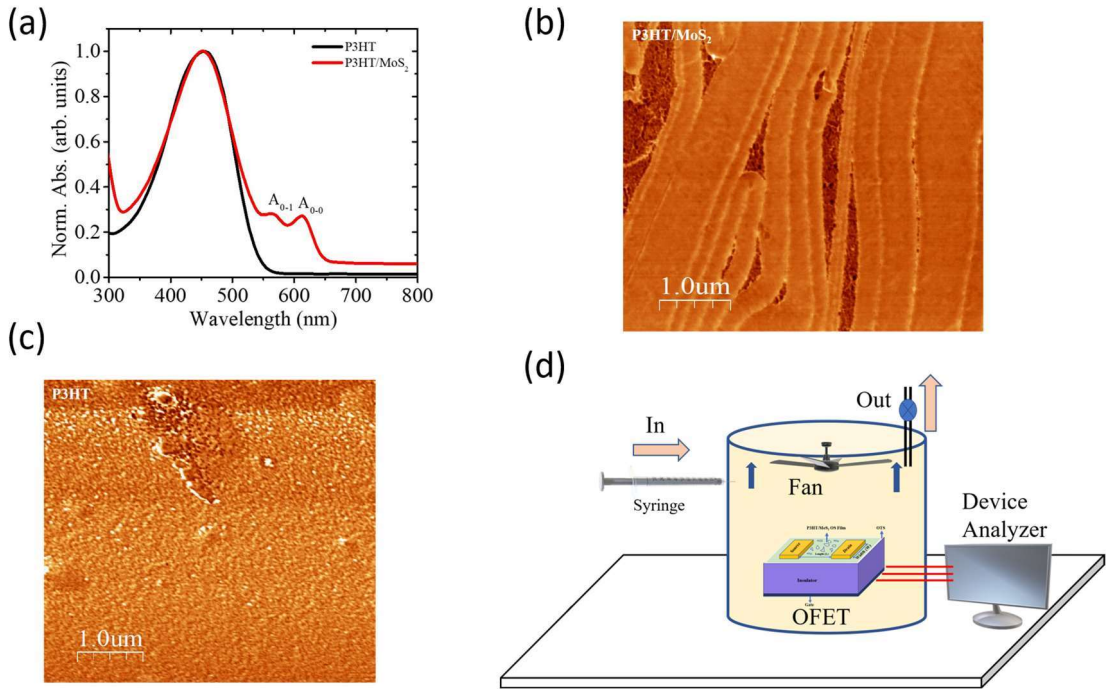

Figure 2.3 (a) Optical absorbance spectra of FTM film, Tapping mode AFM image of (b) P3HT/MoS_2 FTM film, (c) pristine P3HT FTM film, (d) Sensing setup for gas sensing devices.

The electrical characteristics measurements of the OTFT utilizing common source configuration in ambient conditions (RT and humidity 54%) and the ambient conditions have been maintained throughout the whole characterization.

2.5 Device Results and Sensing Mechanism

The operating voltages needed for OTFT operation depend mainly on the suitable selection of dielectric, the nature of the exposed analyte, OSC (organic semiconductor channel) material, and its thicknesses. Here, we have optimized the operating voltages of the OTFT gas sensor for V_{GS} = -60 V and V_{DS} = -60 V. The obtained OTFT characteristics shown are similar to conventional MOSFET characteristics. Here, the drain characteristic (I_{DS}-V_{DS}) of the

fabricated sensor is shown in **Figure 2.4(a)**. In the polymer-based OTFT, the stability of the device is the primary concern. The degradation instability is due to the absorption of a large number of hydrophilic groups in the atmospheric air. The stability of the pristine organic semiconductors can be improved by modifying the side chains or removing the organic polymers' oxidative sites (eliminate -OH groups). The OTS on the insulator layer acts as a dielectric surface modifier, and the P3HT/MoS_2 composite, as a sensing film, passes with high ambient stability.

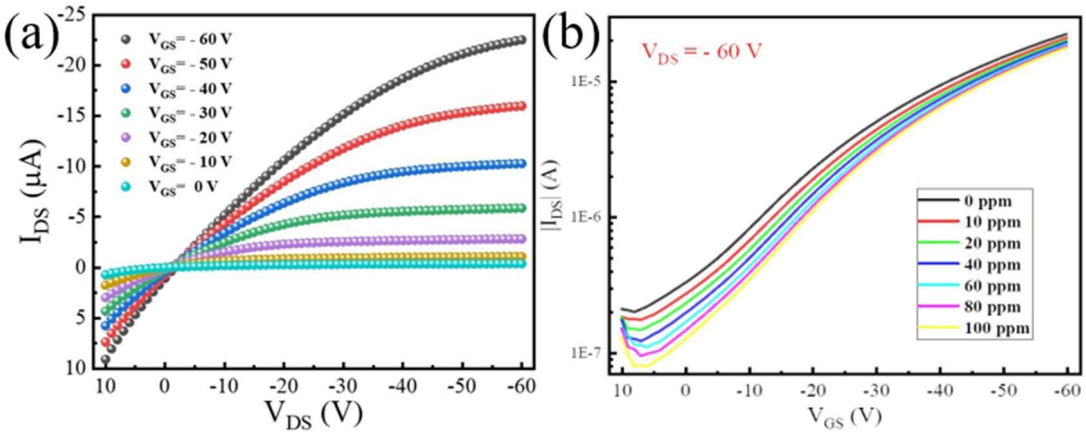

Figure 2.4 (a) Drain characteristics of the P3HT/MoS_2 OTFT, (b) Modulation in the transfer characteristics (I_{DS}-V_{GS} plot) with various concentrations of ammonia gas at V_{DS} = -60 V.

Ammonia gas concentration from the range of 10 to 100 ppm is exposed on the OTFT device, and the change in the drain current (I_{DS}), threshold voltage (V_{TH}), and mobility (μ_p) has been observed. The transfer characteristics plot of the OTFT device for various ammonia concentrations is shown in **Figure 2.4(b).** It is shown that the drain current of the OTFT decreases with the increasing ammonia gas concentration.

The logarithmic plot of change in drain current (I_{DS}) vs. various ammonia concentrations is shown in **Figure 2.5** at V_{DS} = - 60 V and V_{GS} = - 50 V. The plot clearly shows the good linear response of the OTFT device for different ammonia gas concentrations with a correlation

coefficient $R^2 = 0.9964$.

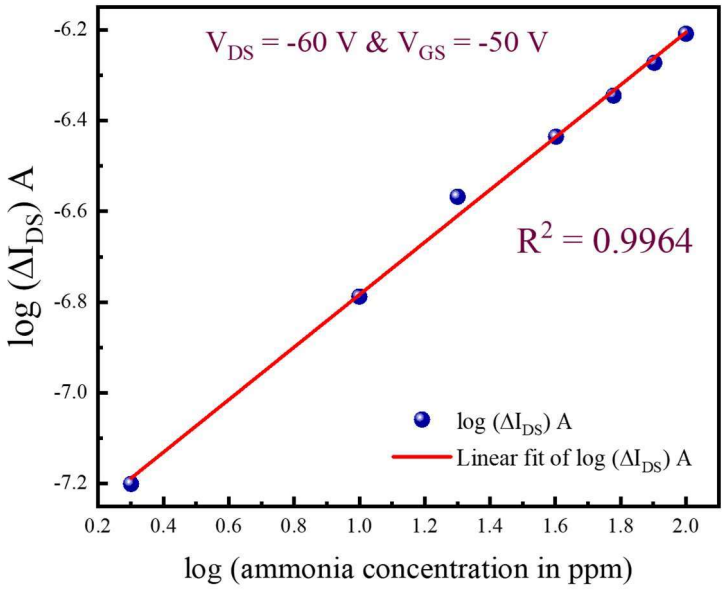

Figure 2.5 Logarithmic plot of change in I_{DS} for various Log concentrations of ammonia.

The threshold voltage and the mobility of the P3HT/MoS_2 composite OTFT can be derived by the drain current (I_{DS}) of the OTFT. The saturation drain current (I_{DS}^{sat}) of the device can be given by-[17]

$$I_{DS}^{sat} = \frac{1}{2}\mu_p C_{OX}\frac{W}{L}(V_{GS} - V_{TH})^2 \; ; \; V_{DS} \geq V_{GS} - V_{TH} \tag{2.1}$$

Where μ_p and C_{ox} are mobility and oxide capacitance, respectively, W/L represents aspect ratio (ratio of width (W) and length (L) of the channel) of the device. The mobility (μ_p) and process aspect ratio (W/L) of the OTFT are very important factors in determining the current-carrying capability of the OTFT under an applied potential. Equation (2.1) can be rewritten as-

$$\sqrt{I_{DS}^{sat}} = \sqrt{\frac{1}{2}\mu_p C_{OX}\frac{W}{L}}\,(V_{GS} - V_{TH}) = \; KV_{GS} - M \tag{2.2}$$

The value of mobility (μ_p), threshold voltage (V_{TH}) can be obtained graphically by linear line

equations given in equations (2.3) & (2.4). The mobility (μ_p) and the threshold voltage of the transistor can be calculated from-

$$\mu_p = \frac{2L}{WC_{ox}} K^2 \quad (2.3)$$

$$V_{TH} = \frac{-M}{K} \quad (2.4)$$

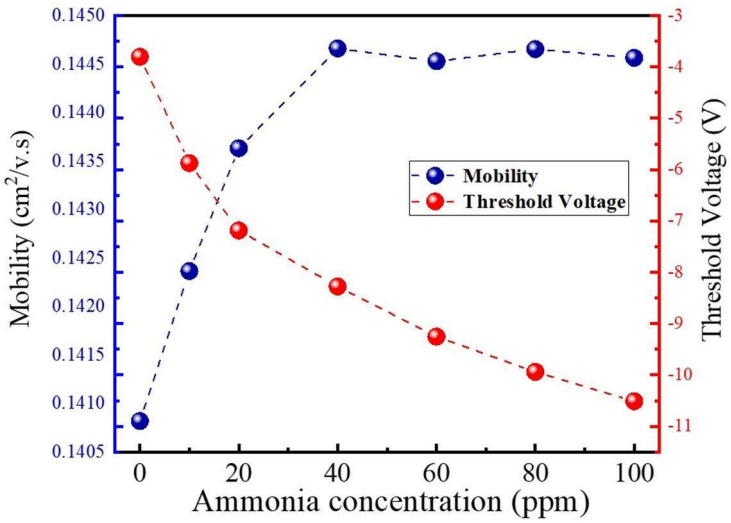

Figure 2.6 Mobility (μ_p) and threshold voltage (V_{TH}) with various ammonia concentrations (0 to 100 ppm).

The negative shifting in threshold voltage with different NH_3 gas concentrations is shown in The threshold voltage (V_{TH}) and mobility (μ_p) with varying concentrations of ammonia analyte are plotted in **Figure 2.6**. Upon ammonia gas exposure, the V_{TH} of the OTFT sensor is displaced in a negative direction from -3.79 V (in the air) to -10.53 V (at 100 ppm). On the other, the mobility of the OTFT sensor is found to be almost constant. There is a minute change of 2.7% in mobility after exposure to a 100 ppm concentration of ammonia gas, increasing from 0.1408 cm^2/V-sec (in ambient) to 0.1446 cm^2/v-sec (at 100 ppm). This shift in the threshold voltage is possible due to the trapped charge near the polymer-dielectric interface. Further, the ammonia (reducing gas) molecule has a tendency to donate its electron pair, where the electron pair of the ammonia molecule reduces the positive charge (hole) of P3HT/MoS_2 composites. It increases the trap charge density and, thereby the space charge

layer. The trap charge density ($Q_{trap.}$) can be calculated by [147]–

$$Q_{trap.} = \frac{\Delta V_{TH} C_{ox}}{q} \tag{2.5}$$

Where 'ΔV_{TH}' *and* 'C_{ox}' represent the change in threshold voltage and oxide capacitance, respectively. The trap charge density increases from 1.895 x 10^{11} /cm^2 to 5.26 x 10^{11} /cm^2 upon the varying concentration of ammonia gas (ambient to 100 ppm). The trap charge density with varying concentrations of ammonia is shown in **Figure 2.7**.

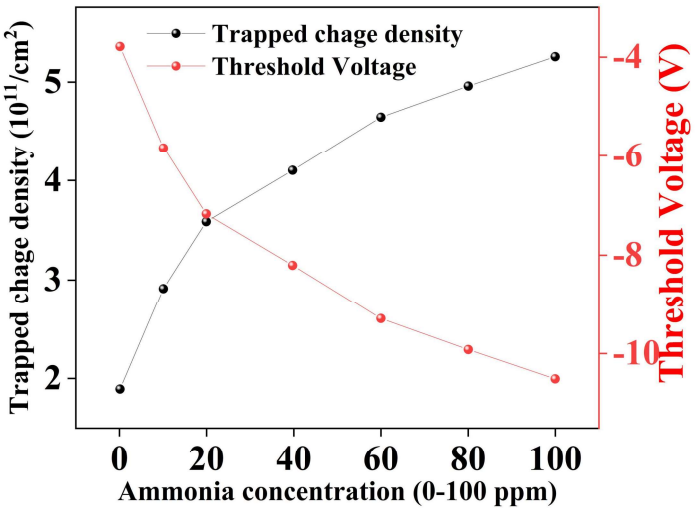

Figure 2.7 Change in the trap charge density with various concentrations of ammonia gas.

2.6 Electrical and Extracted Sensing Parameters

2.6.1. Evolution of Gas Response

To investigate the gas sensing response, the OTFT sensor is exposed to various concentrations of ammonia gas, and a change in device parameters is observed. The sensing response of ammonia gas can be explained by the redox reaction. When any reducing gas, such as ammonia is exposed to the surface of a p-type organic semiconductor, it will extract positive charges (holes) from the surface or donates electrons to the surface. Thereby fewer holes are available for transport, so drain current (I_{DS}) reduces. The modulation observed in the I_{DS} has

been used to determine the sensing response of an OTFT. At a fixed V_{DS}, let us consider I_{Air}, I_{NH3} are the drain current in the presence of air and ammonia gas. Then the sensing response 'S' can be calculated by-[17]

$$S = \frac{|I_{Air} - I_{NH_3}|}{|I_{Air}|} * 100\% \quad (2.6)$$

2.6.2. Sensing Response and Selectivity

The sensing response S of the fabricated sensor device is given in equation (2.6). In the sub-threshold regime of OTFT operation, the ratio of drain current in the air to drain current at various ammonia gas concentrations (0-100 ppm) or sensitivity vs. gate to source voltage (V_{GS}) variation at the fixed drain to source voltage (V_{DS}) is shown in **Figure 2.8(a)**. It shows that the drain current decreases with ammonia concentration. The sensing response at 10 ppm ammonia is 18.20% and increases to 63.45% at 100 ppm. **Figure 2.8(b)** indicates the sensing response for increasing ammonia gas concentration from 0 to 100 ppm. The variation in the different parameters with exposed ammonia is shown in **Table 2.1**. The whole parameter measurement is carried out at room temperature (25 ºC).

The selectivity bar plot for different interfering gases CH_4, CO, CO_2, and NH_3 have been performed for the selectivity analysis of the gas sensor. The sensing response of CH_4, CO, CO_2, and NH_3 at 100 ppm is plotted in **Figure 2.8(c).** The selectivity bar chart clearly shows that the sensing device is highly selective for ammonia gas. In addition to the above, the fabricated OTFT sensor has also been exposed to NO_2 gas and found that this sensor may not suited for NO_2 sensing as it damages the sensing surface swiftly; probably due to the corrosive nature of NO_2 gas [148].

2.6.3. Detection Limit

The detection limit of a gas sensor is another key parameter to check the sensor's performance. This can be extracted from the sensing response curve of the OTFT sensor with varying ammonia concentrations. The theoretical value of the LOD is given by-[17]

$$LOD = \left(\frac{3\,\sigma}{l}\right) \tag{2.7}$$

Where σ represents the root-mean-square deviation of the baseline and the linear fitting of gas response, and 'l' represents the concentration slope, respectively. The slope value is calculated by linear fitting of the sensing plot at low ammonia concentration as it passes with high linearity and high correlation coefficient. The detection limit was found to be 904 ppb for this OTFT sensor.

Table 2.1 Variation in Different Parameters with Exposed Ammonia Gas

Conc. of ammonia gas (ppm)	Threshold voltage (V_{TH}) V	Mobility (μ_p) cm^2/V-sec	Trap Density ($\times 10^{11}$ /cm^2)	Response (S) (%)
0	-3.78	0.1408	1.89	0.00
10	-5.82	0.1423	2.91	18.20
20	-7.17	0.1436	3.58	31.05
40	-8.20	0.1447	4.10	41.79
60	-9.29	0.1446	4.64	51.52
80	-9.92	0.1447	4.96	58.23
100	-10.51	0.1446	5.25	63.45

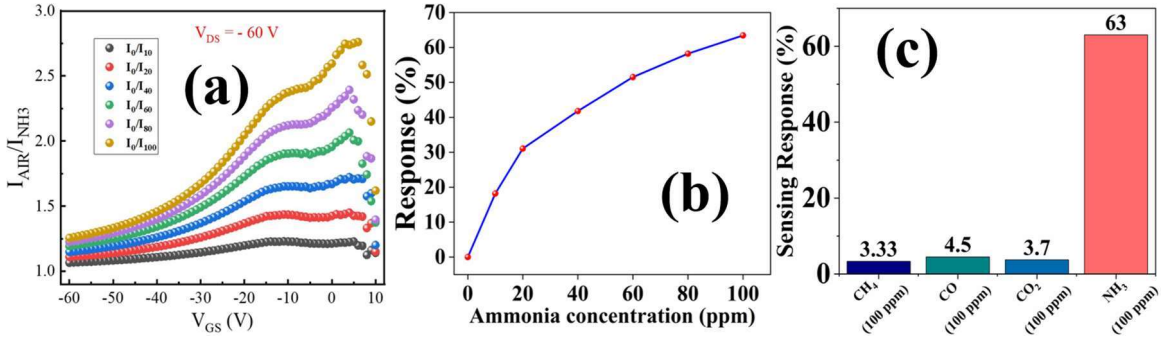

Figure 2.8 (a) I_{Air}/I_{NH3} vs. V_{GS} response for varying ammonia concentration, (b) Sensing response plot for varying ammonia concentration (0-100 ppm), (c) Selectivity plot of P3HT/MoS_2 sensor for CH_4, CO, CO_2, NH_3 gas.

2.6.4. Effect of Relative Humidity Variation

Figure 2.9 shows the effect of humidity on the sensing performance of the gas sensor. **Figure 2.9(a)** shows the sensing performance of the P3HT/MoS_2 sensor slightly decreases with the increase in the relative humidity conditions, but their effect on gas sensing response is negligible. The minimal decrease in the sensing response is probably due to the absorption of water molecules at the surface area and occupying the active area of the sensor. So, there is a slight decrease in the number of active sites for the adsorption/desorption of ammonia molecules, resulting in a minute decrease in the sensing response [149]. The change in the sensing response with relative humidity variation is shown in **Figure 2.9(b)**.

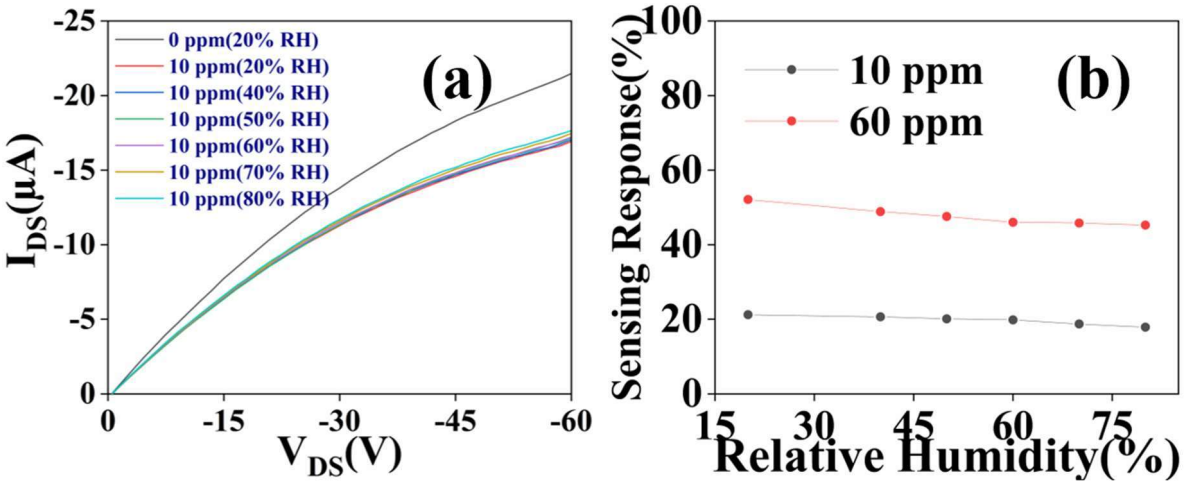

Figure 2.9 Sensing response with variation in relative humidity (a) I_{DS}-V_{DS} (V_{GS} = -60 V) plot at 10 ppm ammonia gas, (b) Sensing response at 10 ppm, 60 ppm with RH variation.

2.6.5. Qualitative Analysis

Qualitative analysis uses subjective judgment about the gas sensor's performance with the help of various measured parameters of the gas sensor. It uses different tangible and inexact information to determine the quality of the gas sensor. The qualitative comparison table is shown in **Table 2.2**. The gas sensor can be classified as MO gas sensors, conductive polymer

sensors, optical sensors, electrochemical sensors, etc. Among them, the MO gas sensor required a high temperature to operate (usually >150 °C). Optical sensors endow costly to set up and are usually limited to monitoring environmental toxic gases. Electrochemical sensors endow low-temperature range and less time span due to chemical properties of sensing film changes on the respective test.

Polymer sensors can be one of two categories (1) Chemiresistive polymer sensors and (2) Conjugative polymer OTFT sensors. Among polymer-based gas sensors, conjugative polymer composites-based OTFTs have a better-amplified sensing response than chemiresistive gas sensors due to an extra gate electrode. The conjugated polymer composite (P3HT/MoS_2), having better stability due to MoS_2, can provide better sensing response, mobility, and low detection limit. The introduction of MoS_2 in P3HT polymer increased the surface-to-volume ratio (S/V) of the sensing film, which is highly desirable as it increases the sensing area of the film. Furthermore, the Floating film transfer method has various advantages over other deposition methods due to low-cost, highly crystalline/oriented SAM film with optimized thickness. Here, FTM deposited P3HT/MoS_2 over OTS film shows nanofiber morphology with a high surface-to-volume ratio, enhancing the sensing characteristics and better sensor response/recovery time of the gas sensor. At last, it can be said that our FTM-deposited conjugated polymer composites pass with low cost, high mobility, better stability, and high sensing performance. The comparison chart with other ammonia sensors is summarized in **Table 2.2**.

Table 2.2 Ammonia Sensors Qualitative Analysis

Device Structure	Sensing Materials	Response S (%)	Deposition Technique	LOD	Remarks [reference]
MSM	PQT-12	8.6% (100 ppm)	Spin cast	300ppb	Poor response [124]
MO sensor	CuO/rGO	9% (6.5 ppm)	Hydrothermal	NA	Poor response [125]
MO sensor	Pt NP/WO_3	72% (1000 ppm)	Thermal evaporation	1 ppm	Costly setup/poor response [127]
Optical sensor	Silver nanowires	NA	Dip cast	1 ppm	Costly setup, not portable [150]
Optical sensor	Sn doped V_2O_5	77.8% (50 ppm)	Spin cast	NA	Costly setup [151]
Chemirestive	ZnO/PPy	75% (100 ppm)	Screen Printing	1 ppm	High LOD [126]
Chemirestive	α Fe_2O_3/GO	15% (20 ppm)	Hydrothermal	10 ppm	Poor response [152]
OTFT	P3HT/PS	52% (50 ppm)	Spin-cast	5 ppm	Low sensitivity [122]
OTFT	P3HT/MoS_2	~14% (20 ppm)	Spray coating	~4 ppm	Poor response [123]
Our Report	P3HT/MoS_2	31.5% (20 ppm)	FTM	904 ppb	High response/mobility

2.7 Sensing Mechanism

The sensing/interaction mechanism of P3HT/MoS_2 can be broadly explained by the charge trapping and doping/de-doping phenomenon of the active area, as shown in **Figure 2.10 (a-b).** The presence of MoS_2 in the pristine P3HT may enhance the interchain ordering, conjugation length, and crystallization property of the P3HT/MoS_2 nanocomposite film. The enhancement in the crystalline property of the conductive polymer/MoS_2 film is inter-dependent on two other prominent absorption peaks (570 nm and 615 nm) (Refer. **Figure 2.3(a)**) incorporated by MoS_2 [134]. Moreover, in addition to enhanced crystallinity, the P3HT/MoS_2 nanocomposite has nanofibrous morphology as compared to the pristine P3HT (smooth morphology). The presence of MoS_2 in the polymeric nanocomposite film provides an additional path between polymer chains for better charge carrier transport; while in the absence of MoS_2, the domains are separated and uncoupled (Refer **Figure 2.3(b-c)**). The quality of nanocomposite film in terms of crystallinity, surface morphology, and charge transfer

characteristics are due to conjugated π - π electron coupling, improving polaron delocalization over channel length, enhancing the charge transport facility, and mobility of the OTFT device [134][153].

The sensing mechanism over the polymer composite matrix can be explained by the charge transport and physisorption phenomenon with the exposed ammonia gas. As a reducing agent, the ammonia donates its lone pair electrons to the composite p-type film or by accepting the holes from the composite polymer matrix. The donated lone pair electrons have a tendency to reduce the free charge carriers available in the channel or increase trap charge carriers on the backbone of polymer composite matrices, thereby decreasing the drain current of the OTFT. In other words, the conductivity modulation is due to ammonia molecules donating their electrons to the LUMO (Lowest Unoccupied Molecular Orbital) level of the composite film, resulting in an increase in the bandgap. This exposed ammonia gas creates an additional LUMO energy level in the energy gap of semiconducting films. The ammonia analyte behaves like an impurity to the composite film, and creates the trap charge carriers by reducing the availability of free charge carriers in the OTFT channel.

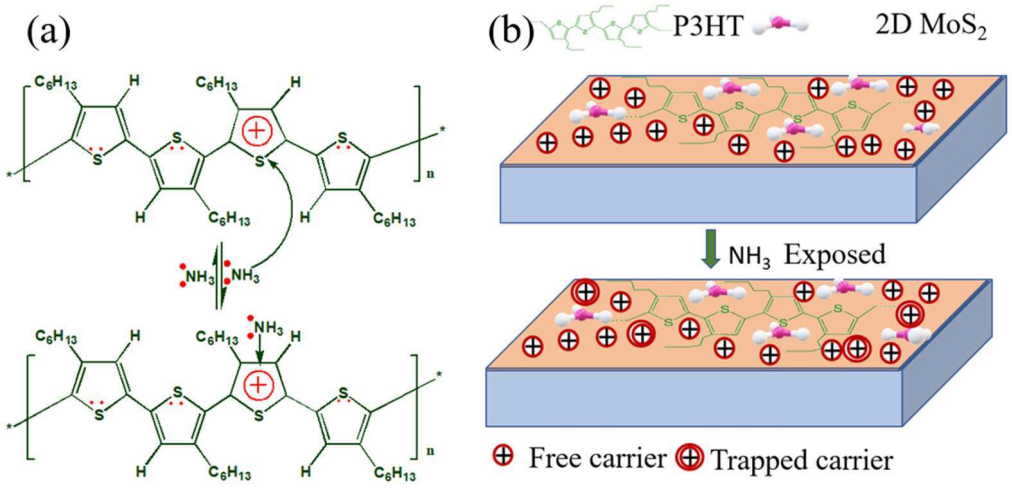

Figure 2.10 (a) Possible interaction of P3HT and ammonia molecule, (b) Sensing mechanism towards ammonia gas.

In the present study, we have investigated the device performance in terms of mobility, threshold voltage, etc. As is already said, ammonia behaves like an impurity to the channel. So, it creates extrinsic defects in the sensing layer and changes the device's threshold voltage (V_{TH}), bandgap, etc. The presence of lone pair electrons of ammonia molecules temporarily changes the charge transfer mechanism across the active channel of the composite matrix. Hence, no permanent changes in the sensing layer have been observed during the test. This is probably due to weak van der Waals forces between the analyte and P3HT/MoS_2 film [154]–[156].

2.8 Conclusion

The fabricated OTFT has various advantages in terms of high efficiency, enhanced performance, better sensitivity, non-invasive, and low-concentration ammonia gas sensor. The superior crystallinity, long conjugation length, and long nanofiber length morphology of the P3HT/MoS_2 surface envisage better charge interaction and transport facilities with analyte ammonia on the sensing surface, thereby enhancing the sensing response of the gas sensor. The OTFT with nanofiber morphology of mobility 0.147 cm^2/Vsec. shows a threshold voltage of -3.78 V (in the air) and changes to -10.71 V after 100 ppm ammonia gas exposure. This ammonia sensor has shown a high sensing response of 63.45% at 100 ppm concentration of ammonia gas. Further, the whole sensing process has been described on the basis of physisorption/weak van der Waals forces between the analyte and P3HT/MoS_2 film. Hence, no permanent changes in the sensing layer have been observed during the test. This OTFT shows that the sensor has better sensing performance and appealing features to sense ammonia gas.